HHS Public Access

Author manuscript

Cell Rep. Author manuscript; available in PMC 2017 February 13.

Published in final edited form as:

Cell Rep. 2016 May 03; 15(5): 968–977. doi:10.1016/j.celrep.2016.03.086.

The kinesin KIF21B regulates microtubule dynamics and is essential for neuronal morphology, synapse function and learning and memory

Mary Muhia[1,6], **Edda Thies**[1,6], **Dorthe Labonté**[1], **Amy E. Ghiretti**[2], **Kira V. Gromova**[1], **Francesca Xompero**[3], **Corinna Lappe-Siefke**[1], **Irm Hermans-Borgmeyer**[4], **Dietmar Kuhl**[3], **Michaela Schweizer**[5], **Ora Ohana**[3], **Jürgen R. Schwarz**[1], **Erika L.F. Holzbaur**[2], and **Matthias Kneussel**[1]

[1]Department of Molecular Neurogenetics, University Medical Center Hamburg-Eppendorf, Falkenried 94, 20251 Hamburg, Germany

[2]Department of Physiology, University of Pennsylvania School of Medicine, Philadelphia, PA 19104-6085, USA

[3]Department of Molecular and Cellular Cognition, University Medical Center Hamburg-Eppendorf, Falkenried 94, 20251 Hamburg, Germany

[4]Transgenic Animal Unit, University Medical Center Hamburg-Eppendorf, Falkenried 94, 20251 Hamburg, Germany

[5]Morphology Unit, Center for Molecular Neurobiology, ZMNH, University Medical Center Hamburg-Eppendorf, Falkenried 94, 20251 Hamburg, Germany

SUMMARY

The kinesin KIF21B is implicated in several human neurological disorders including delayed cognitive development, yet it remains unclear how KIF21B dysfunction may contribute to pathology. One limitation is that relatively little is known about KIF21B-mediated physiological mechanisms. Here, we generated *Kif21b* knockout mice and used cellular assays to investigate the relevance of KIF21B in neuronal and *in vivo* function. We show that KIF21B is a processive motor, and identify an additional role for KIF21B in regulating microtubule dynamics. In neurons lacking KIF21B, microtubules grow more slowly and persistently, leading to tighter packing in dendrites. KIF21B-deficient neurons exhibit decreased dendritic arbor complexity and reduced spine density, which correlate with deficits in synaptic transmission. Consistent with these observations, KIF21B-null mice exhibit behavioral changes involving learning and memory

Correspondence to: Matthias Kneussel.

[6]Equal contribution

AUTHOR CONTRIBUTIONS

D.L., I.H.B., C.L.S. and E.T. generated and verified the KO mouse. M.M. performed and analyzed the behavioral experiments. M.M. analyzed cell biological and electrophysiological data and performed the statistical analysis. E.T. performed and analyzed the neuronal and synaptic morphology data, biochemical western blot-based assays, neuronal motility assays and MT dynamics assays. A.E.G and E.L.F.H. performed and analyzed the in vitro single molecule motility assay. K.V.G. performed and analyzed the TIRF imaging of MTs. J.R.S performed and analyzed the whole cell patch clamp recordings. F.X., O.O. and D.K. performed and analyzed the in vitro field recordings. M.S. performed the electron microscopy analysis. M.K designed the study, analyzed data and wrote the manuscript with the help of M.M and E.T.

deficits. Collectively, our study provides insight into the cellular function of KIF21B and the basis for cognitive decline resulting from KIF21B dysregulation.

Keywords

Neuron; Dendrite; Microtubule dynamics; Kinesin; KIF21B; LTP; Spine; Synapse; Learning and Memory

INTRODUCTION

Kinesin superfamily proteins (KIFs) share a common ATP-binding “motor” domain, fused to divergent tail domains that specify intracellular localization and function. Many kinesins utilize chemical energy derived from ATP hydrolysis to propel directional transport of various cargoes along the microtubule (MT) cytoskeleton (Hirokawa et al., 2009). Kinesins have also been shown to regulate MT dynamics. For example, kinesin-4 and -8 family members adopt dual roles as cargo translocators and regulators of MT dynamics (Drummond, 2011; Walczak et al., 2013). These findings highlight a kinesin-MT interplay in mediating intracellular cargo transport (Hirokawa et al., 2009).

MTs are composed of α- and β-tubulin, and bind specific protein complexes at their plus- and minus- ends (Jiang and Akhmanova, 2011; Yau et al., 2014). The plus-ends of cellular MTs can dynamically remodel through stochastic length fluctuations. These events, termed as dynamic instability, comprise periods of persistent MT growth interrupted by occasional rapid shrinkage: switching between these states of growth and shortening is termed catastrophe and rescue (Gardner et al., 2013).

Studies from several mouse mutant lines have unraveled essential roles for kinesins and other MT binding proteins in neuronal development, survival and higher brain function. Further, abnormalities in kinesin function and the MT cytoskeleton are reflected in a wide spectrum of human diseases, including neurodegeneration and cognitive disability (Franker and Hoogenraad, 2013; Hirokawa and Tanaka, 2015).

Kinesin-4 family members, KIF21A and KIF21B were previously described to share little identity with other KIFs beyond the conserved motor domain, suggesting that they may play unique roles *in vivo* (Marszalek et al., 1999). KIF21A is expressed ubiquitously, and displays robust processive activity *in vitro* (Cheng et al., 2014). KIF21A binds to KANK1 (*ANKRD15*, KN motif and ankyrin repeat domains 1) and co-clusters with liprins and components of the MT attachment complex at the cellular cortex. It inhibits MT growth and engages in organizing MT arrays at the cell edge (van der Vaart et al., 2013). By contrast, KIF21B protein expression is restricted to the brain, spleen and testes (Marszalek et al., 1999). Within neurons, KIF21B is present in axons and dendrites, with particular enrichment in growth cones of developing neurons (Huang and Banker, 2012; Marszalek et al., 1999). KIF21B binds E3 ubiquitin ligase TRIM3 (tripartite motif protein 3) to regulate $GABA_A$ receptor surface delivery (Labonte et al., 2014; Labonte et al., 2013). Micro-duplications in the chromosomal region 1q32.1, including the *Kif21b* gene, have been described in individuals with delayed motor and cognitive development (Olson et al., 2012). Additionally,

polymorphisms in the *Kif21b* gene have been identified as a susceptibility locus for Multiple Sclerosis (MS) Goris et al., 2010; International Multiple Sclerosis Genetics, 2010). More recently, KIF21B enrichment was linked to accelerated neurodegeneration in MS and Alzheimer´s disease (AD). Indeed, its expression was increased several-fold in MS and AD patients at different ages and disease severity Kreft et al., 2014).

Despite this potential clinical relevance, it is currently unclear how KIF21B dysfunction contributes to neuropathology, largely because the physiological function of KIF21B is not yet understood. Thus, insight into KIF21B-mediated mechanisms is instrumental in elucidating its influence on neuronal health. To this end, we generated a *Kif21b* knockout mouse and employed cellular assays of KIF21B depletion and overexpression in order to investigate its functional significance in cytoskeletal transport, neuronal integrity, and behavior. We show that KIF21B is a processive kinesin motor that also regulates MT dynamics. We identify a neuronal role for KIF21B in dendritic tree branching and spine formation, and show that KIF21B is necessary for learning and memory. Overall, our studies characterize the function of KIF21B in neurons and provide insight into its role in cognition.

RESULTS

Generation and verification of *Kif21b* knockout (−/−) mice

To investigate the *in vivo* relevance of KIF21B, we generated *Kif21b* knockout (−/−) mice (Figure 1A) using knockout first embryonic stem (ES) cells obtained from the Knockout Mouse Project repository (KOMP, clone No. 24702). Successful gene targeting was confirmed using Southern blotting and PCR analysis (Figures 1B–D). Western blot experiments using a KIF21B-specific antibody (Figures S1A–B) confirmed loss of KIF21B in −/− mice (Figure 1E). Relative to +/+ controls, immunohistochemical staining revealed the absence of detectable KIF21B signal above background levels in −/− brain tissue (Figure 1F, Figure S1C). Thus, the targeting approach was effective in constitutively abolishing *Kif21b* gene expression in −/− mice without changing KIF21A expression levels (Figure S1D–E). This allowed us to investigate the influence of KIF21B on neuronal development, network integrity, and subsequent impact on adult behavior. *Kif21b* −/− mice were viable and showed no overt abnormalities (Figures S1F–G). Examination of Nissl-stained −/− brain sections revealed normal hippocampal structure (Figures 1G–H), and intact cortical lamination indistinguishable from +/+ controls (Figures 1I–J). Further evaluation in young and aged *Kif21b* +/+ and −/− brains revealed no discernable changes in astrogliosis (not shown) or neurodegeneration (Figure S1H).

Kif21b −/− mice exhibit learning and memory deficits

Whilst kinesins KIF17 and KIF1A have been implicated in learning and memory (Kondo et al., 2012; Wong et al., 2002; Yin et al., 2011), the involvement of other KIFs in cognition remains largely unexplored. On this basis, we sought to address the impact of *Kif21b* ablation on learning and memory processes. Assessment in a novel open field arena revealed intact locomotor activity and habituation in −/− mice (Figure S1I). However, in the Morris water maze reference memory test, −/− mice displayed inferior spatial acquisition relative to +/+ controls. Despite improving across training, −/− mice showed significantly longer

latencies and distance to reach the goal platform (Figures 1K–M). This impairment was limited to acquisition since both genotype groups demonstrated a focused preference for the target quadrant the absence of the platform (Figure 1N). Hence, KIF21B depletion may interfere with the initial encoding of spatial information but may not be critical for spatial memory retrieval or retention.

To investigate whether this learning deficit translated to other cognitive domains, we tested the mice for cued conditioned fear memory. *Kif21b* −/− mice displayed comparatively weaker freezing responses to the tone conditioned stimulus (CS) during acquisition (Figure 1O). Upon re-exposure to the training context, both genotype groups exhibited comparable freezing levels (Figure 1P), suggesting that memory of background contextual cues is unaltered in −/− mice. We then examined the freezing response elicited by the CS by focusing on the first 30 s, when the length of the tone corresponds to that used during acquisition. Here, −/− mice showed significantly less freezing compared with +/+ controls (Figure 1Q). Furthermore, the freezing response to the entire 8 min tone (extinction) was significantly decreased in −/− mice (Figure 1R). Thus, acquisition and memory of the tone CS was impaired in −/− mice. Together, these data indicate that KIF21B is critical for learning and memory function.

KIF21B depletion alters neuronal dendritic tree branching and spine formation

Adaptive changes in the structural and functional properties of neurons and neuronal networks are considered to represent the cellular basis for some forms of learning and memory (Bliss and Collingridge, 1993; Martin et al., 2000). Cognitive disturbances in *Kif21b* −/− mice may therefore stem from abnormalities in cellular and network morphology, or synaptic transmission. To this end, we examined long-term potentiation (LTP) and long-term depression (LTD) at hippocampal Schaffer collateral synapses. Theta burst stimulation (TBS) induced strong and long-lasting LTP in slices derived from +/+ and −/− mice (Figure S2A). Similarly, a low frequency stimulation protocol induced stable LTD in both genotype groups (Figure S2B). We then examined LTP using high frequency stimulation (HFS), which evoked a long lasting LTP in both +/+ and −/− slices. However, we observed a moderate attenuation in early-LTP from −/− slices ($p = 0.08$), suggestive of possible changes in induction of plasticity (Figures 2A, S2C).

We examined neuronal morphology by first assessing dendritic arbors from Dil-labeled CA1 pyramidal cells. Sholl analysis of reconstructed neurons (Figure 2B) revealed altered dendritic tree complexity in −/− neurons, corresponding to significantly less branching in both basal and apical dendrites (Figure 2C). Furthermore, the density of mushroom-type spines on apical dendrites (Figures 2D–E), and stubby-type and total spines on basal branches was significantly decreased in −/− neurons (Figures 2F–G). Ultrastructural examination revealed intact postsynaptic densities (PSDs) in *Kif21b* −/− spines (Figure S2D–E), indicating that the morphology of existing spines remains unaltered.

We observed similar changes in spine density in cultured hippocampal *Kif21b* −/− neurons (Figure 2H, I), and in cultured +/+ neurons following acute KIF21B shRNA knockdown (Figure S2F). In contrast to observations on KIF21B, we found that acute KIF21A knockdown did not alter spine density in +/+ neurons nor exacerbate the spine phenotype in

Kif21b −/− neurons (Figure S2G). Thus, the observed decrease in spine density is specific to KIF21B.

Since reductions in spine density might alter synapse function, we performed cell surface biotinylation experiments to assess for possible changes in the levels of synaptic membrane proteins. The cell surface levels of AMPA receptor (AMPAR), $GABA_A$ receptor ($GABA_AR$) subunits, and a neuroligin (Figure 2J and Figure S2H), but not their total protein content (Figure 2K and Figure S2I), were reduced in *Kif21b* −/− slices, suggesting a general reduction in synapse numbers. Accordingly, analysis of AMPAR-mediated spontaneous excitatory postsynaptic currents (EPSCs) revealed prolonged inter-event intervals in −/− neurons (Figure 2L–M and S2J). However, the mEPSC amplitudes and mean current densities remained unchanged (Figures 2N, S2K) indicating that remaining synapses are functional. These observations were specific, since action potential properties were similar for both groups (Figures S2L–N), confirming that neurons were in a healthy condition. Together, these findings indicate that KIF21B is essential for the development of dendritic arbors, synapse number, and corresponding cell surface expression of individual synaptic proteins.

KIF21B displays processive activity

KIFs play a major role in neuronal function via their ability to propel cargo along the MT cytoskeleton (Hirokawa et al., 2009). To gain mechanistic insight into the sub-cellular role of KIF21B, we first examined its kinetic properties by employing an *in vitro* single molecule motility assay. We characterized KIF21B motor activity using a Halo-tagged truncated form of the kinesin (KIF21B (1-657)), which lacks C-terminal residues that may be involved in autoinhibition. The movement of Halo-tagged KIF21B (1-657) could be visualized along Taxol-stabilized GFP-labeled MTs (average MT length: 45.6 μm). We found KIF21B to be processive, with run lengths of nearly 10 μm (average velocity = 0.43 μm/sec; average run length = 8.8 μm). KIF21B particles remained on the MT for an average of 26.5 s before completing their runs and falling off (Figures 3A, left and 3B–C). To exclude the possibility that the observed mobility may stem from hitchhiking on alternative motors, we introduced a point mutation in the motor domain KIF21B (1-657) T96N. The presence of the T96N mutation completely abolished particle mobility compared with the control fusion protein (KIF21B (1-657); Figure 3A, right), indicating that KIF21B moves processively independent of other drivers. In +/+ neurons, we used a similar construct (mCherry-KIF21B (1-620)), which also revealed frequent mobile particles. Particles moved bi-directionally interspersed with pauses, at an average velocity of 0.4 μm per sec (Figures 3D–E). Thus, KIF21B displays processive activity both *in vitro* and in neurons.

KIF21B regulates MT dynamics

Kinesin-4 family motors, including KIF21A, have been shown to regulate MT dynamics (Bringmann et al., 2004; van der Vaart et al., 2013). Since KIF21B shares 61% identity with KIF21A (Marszalek et al., 1999), KIF21B might also act to regulate MT dynamics. To test this hypothesis, we used the MT-plus end binding protein EB3 to image the growth of MTs in HeLa cells expressing full length KIF21B, KIF21B (1-620) or KIF21B (T96N) fluorescent fusion proteins (Figures 3F). Overexpressed full length KIF21B significantly

increased MT growth rates (Figure 3G–H), whereas all fusion proteins, independent of the C-terminal truncation or the functional mutation in the motor domain, decreased the growth of +TIP-labeled MTs (Figure 3I and Figure S3A). Thus, it appears that KIF21B motility may not be necessary for its ability to regulate MT growth.

We further employed TIRF imaging and examined mRFP-α-tubulin labeled MTs in HeLa cells. Full length KIF21B, but not GFP-KIF21B (1-620) decreased the average MT lifetime prior to catastrophe (Figure 3J and Figure S3B), independent of changes in tubulin posttranslational modifications (Figure S3C).

Next, we performed EB3 imaging in neurons, and observed that +TIP-labeled MTs in KIF21B-deficient neurons had significantly slower growth rates. At the same time, the distance of MT growth was substantially longer in −/− neurons, compared with +/+ neurons (Figure 4A–D). Further ultrastructural examination revealed significantly shorter distances and tighter packing between adjacent MTs in *Kif21b* −/− dendrites (Figures 4E–F). Together these data indicate that, in addition to its role as a cargo motor, KIF21B acts by limiting MT growth and influences MT polymerization/de-polymerization rates.

Since MTs serve as cytoskeletal rails for active motor transport, changes in MT dynamics might in turn impact alternative kinesin-driven transport parameters. Therefore, we analyzed mitochondria motility, which is driven by kinesins 1 and 3 (Hirokawa et al., 2009; Lin and Sheng, 2015). Using Mito Tracker imaging, we observed that whereas mitochondria travelled at similar speeds in *Kif21b* +/+ and −/− neurons, the duration of movement was substantially reduced in −/− neurons, indicating that mitochondria travel over shorter distances (Figures 4G–I). Additionally, we observed significantly less stationary mitochondria in −/− neurons (Figure 4J), suggesting that alterations of MT dynamics in KIF21B depleted neurons might induce secondary changes on MT-based transport.

KIF21B regulation of MT dynamics influences spine formation

A central role for MTs in spine formation and morphology is inferred from studies showing that activity-induced changes in MT dynamics lead to transient MT invasion of spines (Gu et al., 2008; Hu et al., 2008; Jaworski et al., 2009). Therefore, we explored the possibility that the observed defects in MT dynamics might contribute to the *Kif21b* −/− neuronal spine phenotype (Figure 2H–I). We re-expressed either full length KIF21B or KIF21B (1-620) to assess their efficacy in normalizing spine number in *Kif21b* −/− neurons. Neurons were analyzed after 48 h to avoid toxicity associated with protein overexpression over extended periods. Despite the modest time window, re-expression of either fusion protein significantly increased the number of filamentous spines. Moreover, full length KIF21B and KIF21B (1-620) induced a partial but significant normalization of the total number of spines above KIF21B knockout background (Figure 4K and Figure S3D). Re-expression of the C-terminal truncated KIF21B (1-620) fragment, which lacks the cargo-binding domain, was sufficient to mediate this effect. These results indicate that KIF21B's regulation of MT dynamics play an important role in spine formation, although it is likely that its role in cargo trafficking may also be involved.

DISCUSSION

The present study aimed to elucidate KIF21B-mediated mechanisms and functional significance in neurons and *in vivo*. We show that KIF21B is highly processive, and together with its known function in MT-dependent transport (Labonte et al., 2014), also identify a role for KIF21B in regulating MT dynamics. Thus, similar to other kinesin-4 family members (Drummond, 2011; Walczak et al., 2013), KIF21B exerts dual functions as a processive motor and MT regulator. However, it differs from KIF21A with respect to MT growth rates (van der Vaart et al., 2013). Unlike KIF21B, acute knockdown of KIF21A gene expression does not alter dendritic spine number (Figure S2G). Therefore, it seems unlikely that the two kinesins are functionally redundant. It is noteworthy that polymorphisms of either motor are implicated in distinct human neurological disorders.

We also identify an integral role for KIF21B in learning and memory, thereby providing further insight into the role of KIFs and their unique cargoes in modulating cognitive function (Kondo et al., 2012; Yin et al., 2011). *Kif21b* −/− mice were selectivity impaired in spatial acquisition but displayed normal spatial memory, which is concomitant with largely intact hippocampal synaptic plasticity. One possibility is that KIF21B deficiency impedes learning by weakening the ability to form associations between spatial cues and the platform location. This view is reflected by the more severe deficits that emerged in associative fear learning. Hence, the relative contribution of KIF21B to memory appears to depend on the nature of the cognitive task (spatial versus emotional), and possibly the impact of KIF21B deficiency on extra-hippocampal substrates that underlie different forms of learning.

In evaluating network and neural correlates of the cognitive phenotype, we found that KIF21B depletion alters neuronal morphology and function by decreasing dendritic tree branching. Existing branches harbored fewer spines accompanied by diminished neuronal mEPSC frequencies. However, it appears that synaptic receptor content in available spines may be sufficient to mediate adult network plasticity and correspond to unaltered mEPSC amplitudes in −/− neurons.

The observed neuronal abnormalities may stem from the developmental influence of KIF21B on neurite outgrowth. Indeed, KIF21B is enriched at growth cones located at neurite tips (Labonte et al., 2013), suggesting that its direct impact on MT dynamics is expected to influence neurite development and synaptogenesis. Dendrite morphogenesis and spine formation undergo dynamic structural remodeling prior to establishment of the network in adulthood (Koleske, 2013). These processes are intimately connected during development and are critically dependent on factors that influence MT dynamics and transport (Coles and Bradke, 2015; Conde and Caceres, 2009). In this regard, there is increasing evidence linking MT dynamics to synaptic function and memory formation. For instance, growing MT plus ends decorated by the +TIP EB3 enter dendritic spines and can modulate spine morphology (Jaworski et al., 2009). Diminished MT turnover and stability is associated with reduced spine density and impaired memory formation (Fanara et al., 2010).

Given that MTs serve as cytoskeletal rails for active motor transport, alterations in MT-dynamics are anticipated to induce secondary changes on MT-based transport. Thus, it is not

surprising that depletion of a MT dynamics regulator, such as KIF21B, affects mitochondria transport driven by alternative motors. Since the two mechanisms are not mutually exclusive (MT dynamics and transport) the phenotypes owing to *Kif21b* gene ablation are likely to stem from altered MT integrity and corresponding changes in MT-based transport parameters.

Impairments in MT dynamics and cytoskeletal transport are a hallmark feature in neurological disorders (Dubey et al., 2015; Franker and Hoogenraad, 2013). The identification of KIF21B in regulating MT dynamics and transport may represent a common mechanism in neurological disorders associated with KIF21B dysfunction. Subcellular consequences of a defective KIF21B-MT interplay may cause deleterious effects in central and peripheral neuronal subtypes that harbor long axons, and which critically depend on cytoskeletal transport. However, we cannot exclude a currently un-identified role for KIF21B in immune disorders because KIF21B is detected in the spleen and other cell types including oligodendrocytes (Dugas et al., 2006).

KIF21B levels are abnormally elevated in MS and AD (Kreft et al., 2014), including a mouse model for AD (Figure S3E–F). Thus, together with our findings on KIF21B depletion, it is apparent that the precise dose of KIF21B is necessary for neuronal function. Since the ratio of stable to dynamic microtubule populations is critical in neurons, complete depletion or chronic several-fold increase of KIF21B will topple this equilibrium, thereby disrupting neuronal integrity. In keeping with this, it would be of interest to examine whether such changes exist on the MT cytoskeleton in induced pluripotent stem (ips) cell-derived neurons from MS and AD patients. Altogether, our data represent an initial step to delineate the mechanisms involving KIF21B-mediated MT dynamics and trafficking in the context of cognitive function, and increased risk for the disorders in which this motor is implicated.

EXPERIMENTAL PROCEDURES

Detailed descriptions of the materials and methods can be found in the Supplemental Experimental Procedures.

Time lapse imaging of microtubule dynamics and mitochondria motility

To examine MT dynamics, DIV10 neurons were transfected with EB3-GFP. For mitochondria analysis, DIV4 neurons were labelled with 100 nM Mitotracker RedCMXRos (Life Technologies, Germany). Time-lapse imaging was performed using a Nikon spinning disc confocal microscope at 1 frame/s for 200 s and 1 frame/2 s, respectively. The speed and growth of EB3-GFP mobile comets and analysis of mitochondria movement were done with ImageJ (NIH, Bethesda, MD, USA).

In vitro single molecule motility assay

Hela cells were transfected with either Halo-tagged KIF21B (1-657) or KIF21B (1-657) T96N. Motility assays with cell extracts were performed as described (Ayloo et al., 2014). Images were captured using a Nikon TIRF system (Perkin Elmer) on an inverted Ti

microscope (5 frames/s for 120 s). Subsequent analysis was done using the ImageJ TrackMate plugin.

TIRF imaging of MTs

HeLa cells were transfected with mRFP-tubulin and GFP, GFP-KIF21B (full length) or GFP-KIF21B (1-620), respectively. Total Internal Reflection Fluorescence (TIRF) microscopy was performed on a Nikon Spinning disc microscope equipped with a Nikon CFI Apo TIRF 100× 1.49 N.A. oil objective and the 561nm laser to visualize MT at the vicinity of the cell cortex. Images were taken every 1s for 300 frames. To assess the stability of MT, the average lifetime of single MTs before catastrophe was quantified. Quantification was done manually using Volocity (Improvision, Waltham, MA).

Whole cell patch clamp recordings

Recordings were conducted on dissociated hippocampal neurons (DIV20–22) at 21–23°C. The Patchmaster software with the EPC-9 patch-clamp amplifier (HEKA, Lambrecht, Germany) was used for stimulation and data acquisition. Recordings with an access resistance <20 MΩ were evaluated using Fitmaster (HEKA), Igor Pro 6.03 (Wavemetrics), Mini Analysis (Synaptosoft, Decatur, GA), and Excel (Microsoft).

Behavioral analyses

Male and female mice were 10–12 weeks old at the time of testing in the water maze and conditioned freezing experiments.

Supplementary Material

Refer to Web version on PubMed Central for supplementary material.

Acknowledgments

We thank S. Hoffmeister-Ullerich for help with genomic PCR, A. Akhmanova for EB3-GFP, R. Tsien for mRFP-α-tubulin and Eva-Maria Mandelkow and A. Sydow for TG4510 mice. Supported by Deutsche Forschungsgemeinschaft (DFG) grants FOR 2419, project KN556/11-1 and GRK1459 project KN556/14592 and the Hamburg Landesforschungsförderung (LFF) to MK.

References

Ayloo S, Lazarus JE, Dodda A, Tokito M, Ostap EM, Holzbaur EL. Dynactin functions as both a dynamic tether and brake during dynein-driven motility. Nature communications. 2014; 5:4807.

Bliss TV, Collingridge GL. A synaptic model of memory: long-term potentiation in the hippocampus. Nature. 1993; 361:31–39. [PubMed: 8421494]

Bringmann H, Skiniotis G, Spilker A, Kandels-Lewis S, Vernos I, Surrey T. A kinesin-like motor inhibits microtubule dynamic instability. Science. 2004; 303:1519–1522. [PubMed: 15001780]

Cheng L, Desai J, Miranda CJ, Duncan JS, Qiu W, Nugent AA, Kolpak AL, Wu CC, Drokhlyansky E, Delisle MM, et al. Human CFEOM1 mutations attenuate KIF21A autoinhibition and cause oculomotor axon stalling. Neuron. 2014; 82:334–349. [PubMed: 24656932]

Coles CH, Bradke F. Coordinating Neuronal Actin-Microtubule Dynamics. Current biology : CB. 2015; 25:R677–R691. [PubMed: 26241148]

Conde C, Caceres A. Microtubule assembly, organization and dynamics in axons and dendrites. Nat Rev Neurosci. 2009; 10:319–332. [PubMed: 19377501]

Drummond DR. Regulation of microtubule dynamics by kinesins. Seminars in cell & developmental biology. 2011; 22:927–934. [PubMed: 22001250]

Dubey J, Ratnakaran N, Koushika SP. Neurodegeneration and microtubule dynamics: death by a thousand cuts. Frontiers in cellular neuroscience. 2015; 9:343. [PubMed: 26441521]

Dugas JC, Tai YC, Speed TP, Ngai J, Barres BA. Functional genomic analysis of oligodendrocyte differentiation. J Neurosci. 2006; 26:10967–10983. [PubMed: 17065439]

Fanara P, Husted KH, Selle K, Wong PY, Banerjee J, Brandt R, Hellerstein MK. Changes in microtubule turnover accompany synaptic plasticity and memory formation in response to contextual fear conditioning in mice. Neuroscience. 2010; 168:167–178. [PubMed: 20332016]

Franker MA, Hoogenraad CC. Microtubule-based transport - basic mechanisms, traffic rules and role in neurological pathogenesis. J Cell Sci. 2013; 126:2319–2329. [PubMed: 23729742]

Gardner MK, Zanic M, Howard J. Microtubule catastrophe and rescue. Curr Opin Cell Biol. 2013; 25:14–22. [PubMed: 23092753]

Goris A, Boonen S, D'Hooghe MB, Dubois B. Replication of KIF21B as a susceptibility locus for multiple sclerosis. Journal of medical genetics. 2010; 47:775–776. [PubMed: 20587413]

Gu J, Firestein BL, Zheng JQ. Microtubules in dendritic spine development. J Neurosci. 2008; 28:12120–12124. [PubMed: 19005076]

Hirokawa N, Noda Y, Tanaka Y, Niwa S. Kinesin superfamily motor proteins and intracellular transport. Nature reviews Molecular cell biology. 2009; 10:682–696. [PubMed: 19773780]

Hirokawa N, Tanaka Y. Kinesin superfamily proteins (KIFs): Various functions and their relevance for important phenomena in life and diseases. Experimental cell research. 2015; 334:16–25. [PubMed: 25724902]

Hu X, Viesselmann C, Nam S, Merriam E, Dent EW. Activity-dependent dynamic microtubule invasion of dendritic spines. J Neurosci. 2008; 28:13094–13105. [PubMed: 19052200]

Huang CF, Banker G. The translocation selectivity of the kinesins that mediate neuronal organelle transport. Traffic. 2012; 13:549–564. [PubMed: 22212743]

International Multiple Sclerosis Genetics, C. Comprehensive follow-up of the first genome-wide association study of multiple sclerosis identifies KIF21B and TMEM39A as susceptibility loci. Hum Mol Genet. 2010; 19:953–962. [PubMed: 20007504]

Jaworski J, Kapitein LC, Gouveia SM, Dortland BR, Wulf PS, Grigoriev I, Camera P, Spangler SA, Di Stefano P, Demmers J, et al. Dynamic microtubules regulate dendritic spine morphology and synaptic plasticity. Neuron. 2009; 61:85–100. [PubMed: 19146815]

Jiang K, Akhmanova A. Microtubule tip-interacting proteins: a view from both ends. Curr Opin Cell Biol. 2011; 23:94–101. [PubMed: 20817499]

Koleske AJ. Molecular mechanisms of dendrite stability. Nature reviews Neuroscience. 2013; 14:536–550. [PubMed: 23839597]

Kondo M, Takei Y, Hirokawa N. Motor protein KIF1A is essential for hippocampal synaptogenesis and learning enhancement in an enriched environment. Neuron. 2012; 73:743–757. [PubMed: 22365548]

Kreft KL, van Meurs M, Wierenga-Wolf AF, Melief MJ, van Strien ME, Hol EM, Oostra BA, Laman JD, Hintzen RQ. Abundant kif21b is associated with accelerated progression in neurodegenerative diseases. Acta neuropathologica communications. 2014; 2:144. [PubMed: 25274010]

Labonte D, Thies E, Kneussel M. The kinesin KIF21B participates in the cell surface delivery of gamma2 subunit-containing GABAA receptors. European journal of cell biology. 2014; 93:338–346. [PubMed: 25172774]

Labonte D, Thies E, Pechmann Y, Groffen AJ, Verhage M, Smit AB, van Kesteren RE, Kneussel M. TRIM3 Regulates the Motility of the Kinesin Motor Protein KIF21B. PLoS ONE. 2013; 8:e75603. [PubMed: 24086586]

Lin MY, Sheng ZH. Regulation of mitochondrial transport in neurons. Experimental cell research. 2015; 334:35–44. [PubMed: 25612908]

Marszalek JR, Weiner JA, Farlow SJ, Chun J, Goldstein LS. Novel dendritic kinesin sorting identified by different process targeting of two related kinesins: KIF21A and KIF21B. J Cell Biol. 1999; 145:469–479. [PubMed: 10225949]

Martin SJ, Grimwood PD, Morris RG. Synaptic plasticity and memory: an evaluation of the hypothesis. Annual review of neuroscience. 2000; 23:649–711.

Olson HE, Shen Y, Poduri A, Gorman MP, Dies KA, Robbins M, Hundley R, Wu B, Sahin M. Micro-duplications of 1q32.1 associated with neurodevelopmental delay. European journal of medical genetics. 2012; 55:145–150. [PubMed: 22266072]

van der Vaart B, van Riel WE, Doodhi H, Kevenaar JT, Katrukha EA, Gumy L, Bouchet BP, Grigoriev I, Spangler SA, Yu KL, et al. CFEOM1-associated kinesin KIF21A is a cortical microtubule growth inhibitor. Developmental cell. 2013; 27:145–160. [PubMed: 24120883]

Walczak CE, Gayek S, Ohi R. Microtubule-depolymerizing kinesins. Annu Rev Cell Dev Biol. 2013; 29:417–441. [PubMed: 23875646]

Wong RW, Setou M, Teng J, Takei Y, Hirokawa N. Overexpression of motor protein KIF17 enhances spatial and working memory in transgenic mice. Proc Natl Acad Sci U S A. 2002; 99:14500–14505. [PubMed: 12391294]

Yau KW, van Beuningen SF, Cunha-Ferreira I, Cloin BM, van Battum EY, Will L, Schatzle P, Tas RP, van Krugten J, Katrukha EA, et al. Microtubule minus-end binding protein CAMSAP2 controls axon specification and dendrite development. Neuron. 2014; 82:1058–1073. [PubMed: 24908486]

Yin X, Takei Y, Kido MA, Hirokawa N. Molecular motor KIF17 is fundamental for memory and learning via differential support of synaptic NR2A/2B levels. Neuron. 2011; 70:310–325. [PubMed: 21521616]

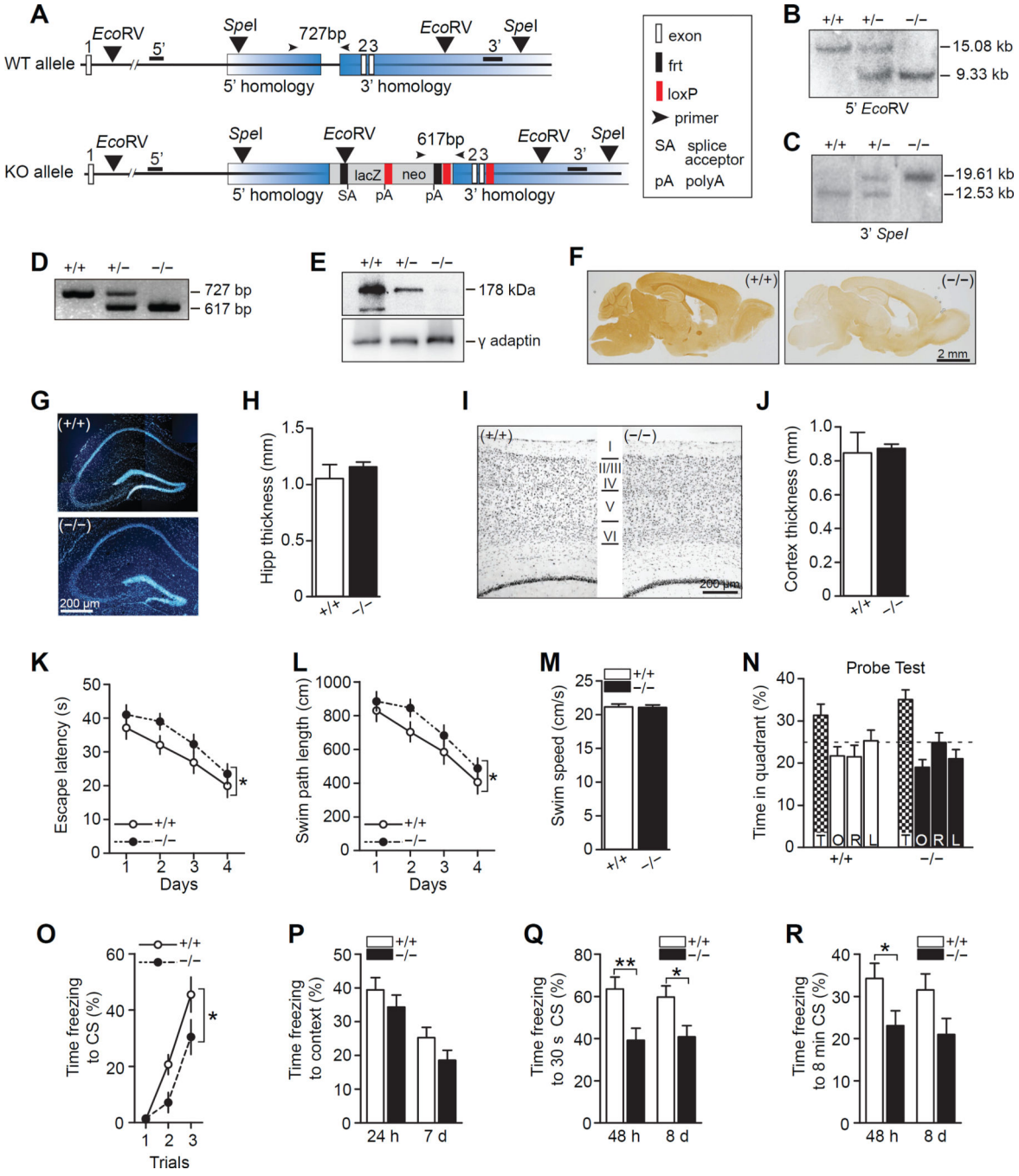

Figure 1. Targeting of the *Kif21b* gene and learning and memory deficits in *Kif21b* −/− mice

(A) Scheme of targeting strategy. Southern restriction sites (*EcoRV* and *SpeI*: 5` and 3´), location of respective probes and PCR primer locations are indicated. KO alleles harbor three *LoxP* sites flanking the neo cassette and exons 2–3 of the *Kif21b* gene coding sequence. The targeting cassette is flanked by frt sites. Integration of the targeting vector results in a knockout-first allele.

(B–C) Southern blot analysis of genomic DNA with 5`- and 3´-flanking probes.

(D) PCR genotyping in +/+, +/− and −/− mice.

(E) Western blot analysis probed with anti-KIF21B and anti-γ-adaptin (loading control).
(F) Immunohistochemical staining confirming loss of KIF21B immunoreactivity in −/− brain tissue.
(G–H) DAPI stain showing grossly normal hippocampal structure (G) and thickness (H) in −/− mice. p=0.67.
(I–J) Nissl stain showing intact cortical lamination (I) and thickness (J; p=0.91) in −/− mice. Student´s t-test. (+/+): n=4, (−/−): n=3.
(K–N) Morris water maze test. Acquisition, as indexed by escape latency (K) and path length (L) to goal platform differs between genotypes. (M) Comparable swim speed for both groups across training (Genotype: p=0.98). (N) Spatial bias for the training quadrant in the probe test. (Genotype: p=0.44). Values represent mean ± SEM (*p < 0.05, Acquisition: RM ANOVA, Probe test: two-way ANOVA, Swim speed: Student's t-test). (+/+) mice: n= (males=6, females=7); (−/−) mice: n=17 (m ales=9, females=8). T: Target, O: Opposite, R: Right, L: Left quadrants.
(O–R) Cued fear conditioning test. (O) Acquisition of conditioned freezing response to the tone CS across three CS-US (tone-shock) pairings. (P) Expression of conditioned freezing response to the background context at 24 h and 7 d after acquisition. (Q) Expression of freezing response to the 30 s tone CS 48 h and 8 d after acquisition. (R) Freezing response to the 8 min CS (extinction) 48 h and 8d after acquisition. Values represent mean ± SEM (*p < 0.05, **p < 0.01: RM ANOVA or two-way ANOVA with post-hoc comparisons). (+/+) mice: n=15 (males=8, females=7); (−/−) mice: n=15 (males=9, females=6)]. See also Figure S1.

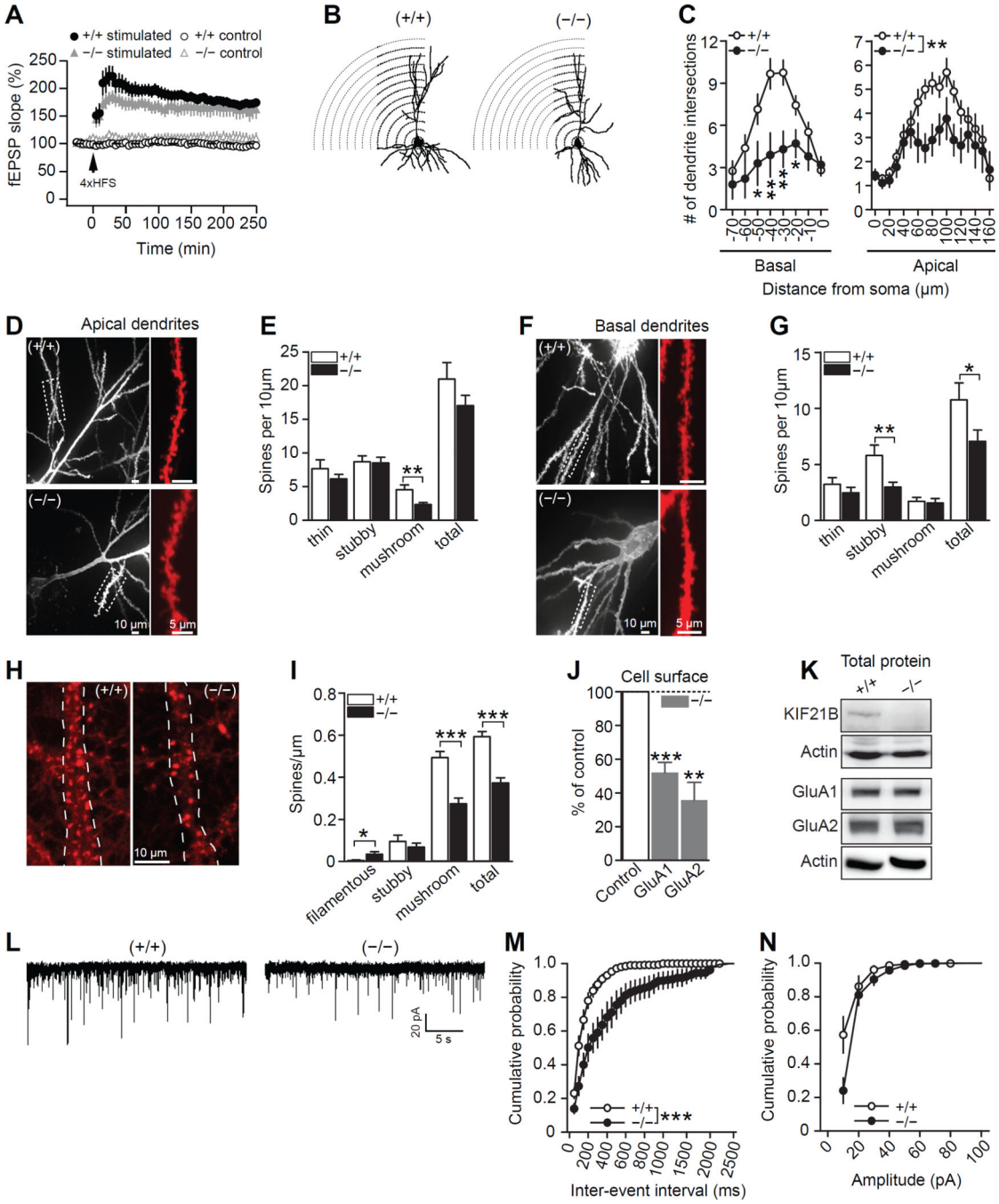

Figure 2. KIF21B deficiency alters neuronal morphology and synaptic function

(A) HFS-LTP (4×, arrow) at Schaffer collateral synapses. ANOVA, (+/+): n=12, (−/−): n=12. (B–C) Diolistic (Dil) dye labeling and imaging in hippocampal slices. (B) Traces of reconstructed dendritic arbors. (C) Sholl analysis of dendrite intersections. RM ANOVA and post-hoc comparisons. (+/+): n=10 neurons, (−/−): n=14 neurons.

(D–G) Spines from Dil-labeled CA1 pyramidal cell apical (D) and basal (F) dendrites. Insets, right: enlargements of boxed areas. (E and G) Spine type and density per 10 μm

dendrite length. Student´s t-test. Apical branches: (+/+): n= 8 neurons, (−/−): n= 17 neurons; Basal branches: (+/+): n= 10 neurons, (−/−): n= 16 neurons.

(H–I) Neurons at DIV22 labeled with Phalloidin rhodamine. (I) Spine density per unit length of dendrite. Student´s t-test. (+/+): n=4 neurons, 15 dendrites, (−/−): n=7 neurons, 15 dendrites. Values expressed as mean ± SEM.

(J) Surface biotinylation assay on hippocampal slices. One sample t-test against 100% loading control. n=5–10 experiments.

(K) Total protein content analysis using hippocampi from +/+ and −/− mice. n=3 experiments.

(L–M) Whole-cell patch-clamp recordings in DIV22 neurons. (L) Sample current traces of mEPSCs. Cumulative probability histograms for mEPSC inter-event intervals (M) and amplitidues (N). KS test. (+/+): n=9, (−/−): n=11. All graphs: *p < 0.05, **p < 0.01, ***p < 0.001. See also Figure S2.

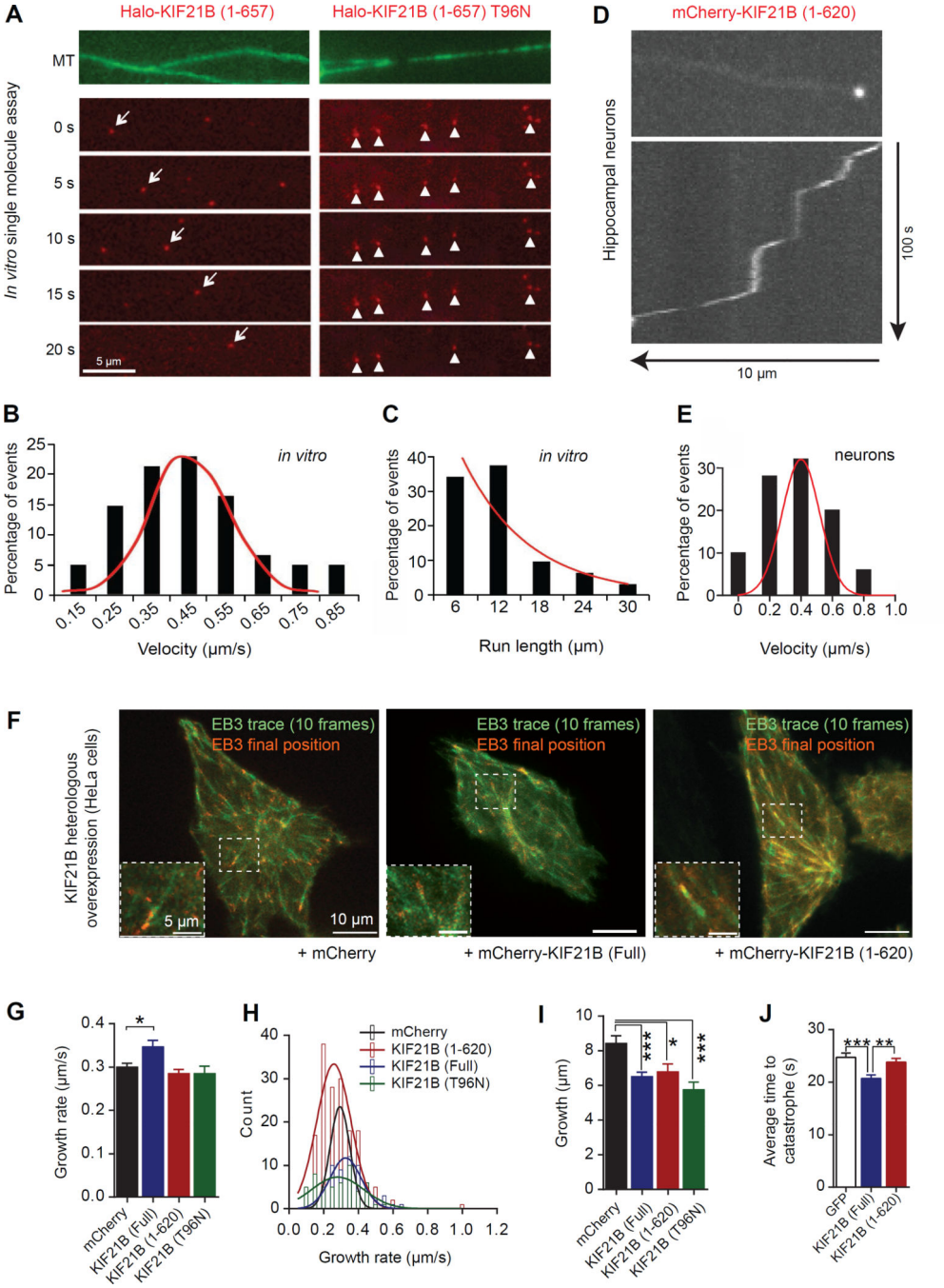

Figure 3. KIF21B is a processive motor and regulates MT dynamics

(A–C) *In vitro* motility assay of single KIF21B particle motility along MTs (left panel) and of KIF21B (1-657) T96N, encoding a point mutation in the motor domain (right panel). The frequency distribution of velocity (B), and run lengths (C) of motile KIF21B particles. Curves represent Gaussian and exponential decay fits, respectively. n=93 particles. (D–E) Time-lapse imaging conducted in neurons transfected with mCherry-KIF21B (1-620). (D) Kymograph illustrating dendritic movement of KIF21B particles. (E) Gaussian distribution and curve fit for particle velocity. n = 23 particles.

(F–I) Time-lapse imaging of +TIP EB3 dynamics in HeLa expressing EB3 together with indicated constructs. 10 consecutive frames were averaged (trace: green). One image was superimposed (final position: red). Insets: enlargements of boxed areas. (G) Average growth rates of EB3 comets in HeLa cells expressing the corresponding constructs. (H) Frequency distribution of comet growth rates. Curves represent Gaussian fits. (I) Average EB3 comet growth in HeLa cells expressing the respective constructs. EB3/mCherry: 7 cells, 69 comets, EB3/mCherry-KIF21B (1-620): 8 cells, 55 comets, EB3/mCherry-KIF21B (Full length): 17 cells, 167 comets, EB3/Halo-KIF21B (1-657) T96N: 8 cells, 51 comets.

(J) TIRF-based live cell imaging of mRFP-α-tubulin labelled MTs in HeLa cells expressing the indicated GFP-fusion proteins. The graph depicts average MT lifetime prior to catastrophe. GFP control: 19 cells, 198 MTs, KIF21B (Full length): 19 cells, 225 MTs, KIF21B (1-620): 20 cells, 224 MTs.

For averaged values (mean ± SEM) (*$p < 0.05$, **$p < 0.01$, ***$p < 0.01$: One-way ANOVA followed by post-hoc comparisons.) See also Figure S3.

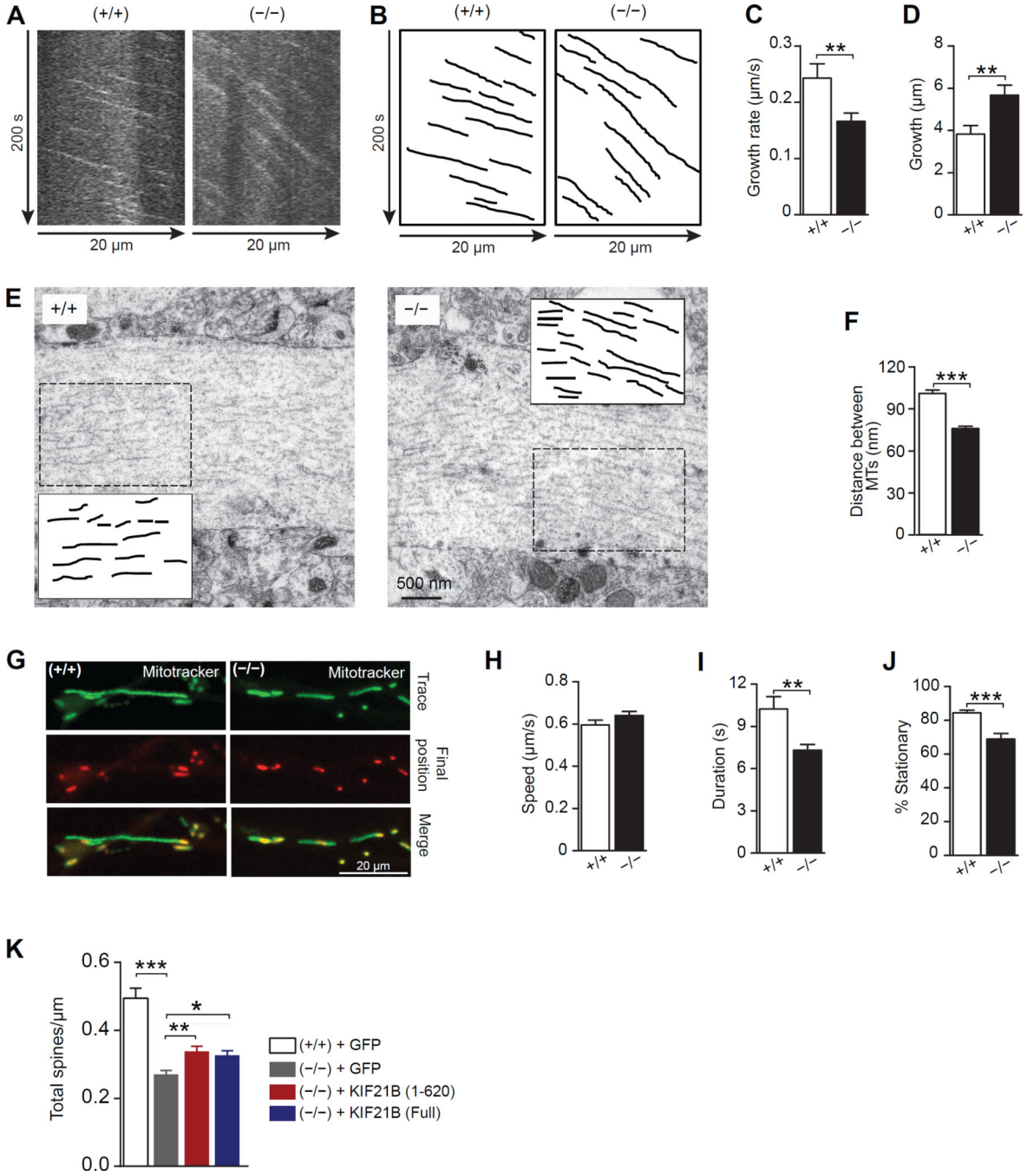

Figure 4. KIF21B depletion affects MT dynamics

(A–D) Neuronal live cell imaging and assessment of +TIP EB3-GFP labeled MT dynamics. (A, B) Kymographs and corresponding traces of EB3-GFP comets illustrating movement (displacement on the x-axis) over time (y-axis). MTs from −/− neurons grow significantly slower (C) but over longer distances (D). (+/+): n=41, (−/−): n=50 comets.

(E–F) Electron micrographs in which MTs were traced (inset rectangles) from dendrites of similar size and orientation. (F) Quantification and analysis of distance between adjacent microtubule traces. (+/+): n=21, (−/−): n=15 dendrites.

(G–J) Neuronal Mitotracker live imaging. (G) 30 consecutive frames (1 sec/frame) were averaged (green trace), and the final position superimposed (red). Graphs depict mitochondria speed (H), duration of movement (I), and number of stationary particles (J). (+/+): n=98, (−/−): n=141 particles.

(K) Quantification of spine number per μm dendrite in hippocampal neurons at DIV 10 transfected with KIF21B (Full length) and KIF21B (1-620) fusion proteins. 10–12 neurons per transfected construct. (+/+) + GFP: 18 dendrites, (−/−) + GFP: 23 dendrites, (−/−) + KIF21B (1-620): 57 dendrites, (−/−) + KIF21B (Full length): 47 dendrites.

All values represent mean ± SEM (*$p < 0.05$, **$p < 0.01$, ***$p < 0.001$: Students t-test and One-way ANOVA followed by post-hoc comparisons.) See also Figure S3.